



The effect of surgery on patellar tendinopathy: Novel use of MRI questions the exploitability of the rat collagenase model to humans



Michael J. Dan^{*}, Rema A. Oliver, James D. Crowley, Vedran Lovric, William C.H. Parr, David Broe, Mervyn Cross, William R. Walsh

Surgical and Orthopaedic Research Laboratories (SORL), School of Clinical Sciences, Faculty of Medicine, University of New South Wales (UNSW), Level 1 Clinical Sciences Building, Prince of Wales Hospital, Gate 6 Avoca Street, Randwick, New South Wales (NSW) 2031, Australia

ARTICLE INFO

Article history:

Received 20 May 2019

Received in revised form 20 October 2019

Accepted 22 October 2019

Keywords:

Patellar tendinopathy

Collagenase

Surgery

Animal model

Rat

ABSTRACT

Background: patellar tendinopathy is an overuse condition most commonly affecting jumping athletes. Surgery is reserved for refractory cases; however, it lacks high level clinical evidence and basic science to support its use. The purpose of this study was to determine the biomechanical and histological response of surgical excision on patellar tendinopathy in the rat collagenase tendinopathy model and correlate MRI findings.

Methods: Forty-eight Long Evans rats were divided into three groups: i) no patellar tendinopathy with surgical excision, ii) patella tendinopathy with surgical excision, and iii) patellar tendinopathy with no surgical excision. Endpoints included histology, mechanical testing, and MRI pre- and post-surgical intervention at one and four weeks.

Results: No difference in failure load or histological grading was seen between the groups at all time points. MRIs showed initial loss of tendon continuity followed by complete healing with elongated and thickened tendons in all groups.

Conclusions: While other research has reported immunohistochemistry and histology of collagenase-induced tendinopathy may be correlated with human pathogenesis, the novel MRI findings from our study suggest that the rat collagenase tendinopathy surgical model may be limited when extrapolating to humans. Further work is needed to determine if any correlation exists between the dosing, location, and animal effect of the collagenase injection model with MRI findings. This is needed before any collagenase model can be used to determine the effect of surgery in the pathogenic response to patella tendinopathy.

© 2019 Elsevier B.V. All rights reserved.

1. Introduction

Patellar tendinopathy, an overuse condition affecting athletes, carries a poor prognosis with up to 53% of athletes retiring from sport due to the condition [1]. Physiotherapy, load management, and injectables are the main stay of treatment; however, 10% of patients require surgery. Traditionally, surgery involves excision of the diseased portion of the tendon (posterior superior tendon as it inserts onto the patella), with or without drilling the bone to stimulate new blood flow to promote healing [2,3].

The clinical effectiveness of surgery has been questioned by high level clinical evidence. Bahr et al. [4] found no difference in patient outcomes between surgery and physiotherapy in a randomized control trial [4,5]. In comparison, lower level evidence of

^{*} Corresponding author at: Surgical & Orthopaedic Research Laboratories, Prince of Wales Hospital, Level 1, Clinical Sciences Building, Randwick, NSW 2031, Australia.
E-mail address: michaeland@hotmail.com. (M.J. Dan).

case series and case control studies have reported great benefit to surgery [6,7], in keeping with the view that the evidence to support surgery is indirectly proportional to the quality of the study [4]. The basic science supporting surgery is based on placing longitudinal incisions into the Achilles tendon of healthy rabbits that generated an increase in the macroscopic appearance of the tendon, believed to translate to increased tensile strength, leading to the rationale of replacing a 'bad scar' with a 'good scar' [8–10].

Animal models for tendinopathy have been created mechanically (through direct force) or chemically (by injection of collagenase) while the direct correlation to the human pathological condition remains in question. The benefit to mechanically inducing tendinopathy is that it may more closely resemble the pathophysiology of tendinopathy in the human (repetitive overload). These models are limited in that the tendinopathy is not induced in the same location as humans and differences in kinematics are clearly different. Tendinopathy is induced in the mid substance of the tendon rather than the most common area in humans, which is the enthesis at the posterior superior patellar tendon [11–13]. The benefit of the chemical model induced through a collagenase injection is it allows for a reproducible dose-dependent response and is reported to be possible at an anatomical specific location similar to humans [14]. However, the reproducibility of this model remains in question.

Reported results from rat tendinopathy models correlate well with known clinical data in some respects. There is good clinical data to support eccentric loading-based exercise therapy [15,16], along with good animal data to support tendon remodeling through mechano-transduction [17] even though the anatomical locations differ. However, in human patients, loading programs often do not show a benefit when performed during the sporting competition period [18], which correlates to detrimental effects of heavy loading too early after the development of patellar tendinopathy in animals [19].

The effect of surgery on patella tendinopathy at a histological and mechanical level has not been explored in humans or animals [17]. Given that collagenase rat tendinopathy models are often considered reflective of the human condition, this study aimed to investigate the histological and biomechanical effect of surgery on patellar tendinopathy in a rat model and correlate our findings with magnetic resonance imaging (MRI).

2. Methods

2.1. Animals

After approval of the Institutional Animal Care and Ethics Committee (ACEC approval 18/51A, UNSW, Australia), 48 female Long Evans rats (Biological Research Centre, Sydney, Australia), weighing on average 220 g, were equally divided and randomly assigned to three groups: i) no patellar tendinopathy with surgical excision, ii) patellar tendinopathy with surgical excision, and iii) patellar tendinopathy with no surgical excision. For those assigned to the tendinopathy group, collagenase was injected into the posterior superior patellar tendon bilaterally. Surgical excision was performed one week later. The same intervention and investigation were performed bilaterally in the same rat. Half the rats were then allocated for histological and MRI endpoints, whereas the other half were allocated solely for mechanical testing. Intervention and time points for each group were randomly allocated (Figure 1). Rats were acclimatized within their own groups with a maximum of four rats per cage, housed at 22 °C with 12-h day–night cycle, fed a standard laboratory diet of rat chow (Gordan's Specialty Stockfeeds, NSW, Australia) and water ad libitum. The rats were monitored daily each week post intervention and weighed weekly. Euthanasia was performed via carbon dioxide inhalation.

2.2. Anesthetic and perioperative care

Prior to collagenase injection and surgical excision, anesthesia was applied and maintained via isoflurane inhalation (two to three percent) with oxygen, titrated to effect. Rats were premedicated with buprenorphine 0.01 mg/kg s/c, 26-gauge insulin syringe. Carprofen (two milligrams per kilogram s/c) was administered for post-operative analgesia and inflammation. Buprenorphine was administered for rescue analgesia as indicated. Rats were monitored daily for the first week following surgery, for pain, surgical wound irritation, appetite and behavioral changes.

2.3. Collagenase injection

For rats allocated to groups 2 and 3, at the initial time point T0 (Figure 1), a longitudinal 0.5 cm skin incision was performed directly over the patellar tendon under aseptic conditions. Type I collagenase (sigma 125CDU/mg) one milligram per milliliter dissolved in 30 µl of phosphate-buffered saline (PBS) was injected into the posterior patella tendon using a 29-gauge insulin syringe. The needle was inserted along the length of the patella tendon from inferior portion until the inferior aspect of the patellar bone was felt, the collagenase was injected while slowly withdrawing to maximize placement in the posterior superior part of the patellar tendon to replicate human location. Routine skin closure was performed using a buried cruciate suture using 4-0 braided multi-filament suture (Vicryl) (Figure 2a–d).

2.4. Surgical excision

For rats allocated to groups 1 and 2, at time point 1 (Figure 1), a longitudinal 1.5 cm skin incision was performed directly over the patellar tendon under aseptic conditions. A longitudinal incision was placed either side of the patellar tendon, medially and laterally, before placing the no. 15 blade through the tendon to excise the posterior and proximal 1/3. The procedure was

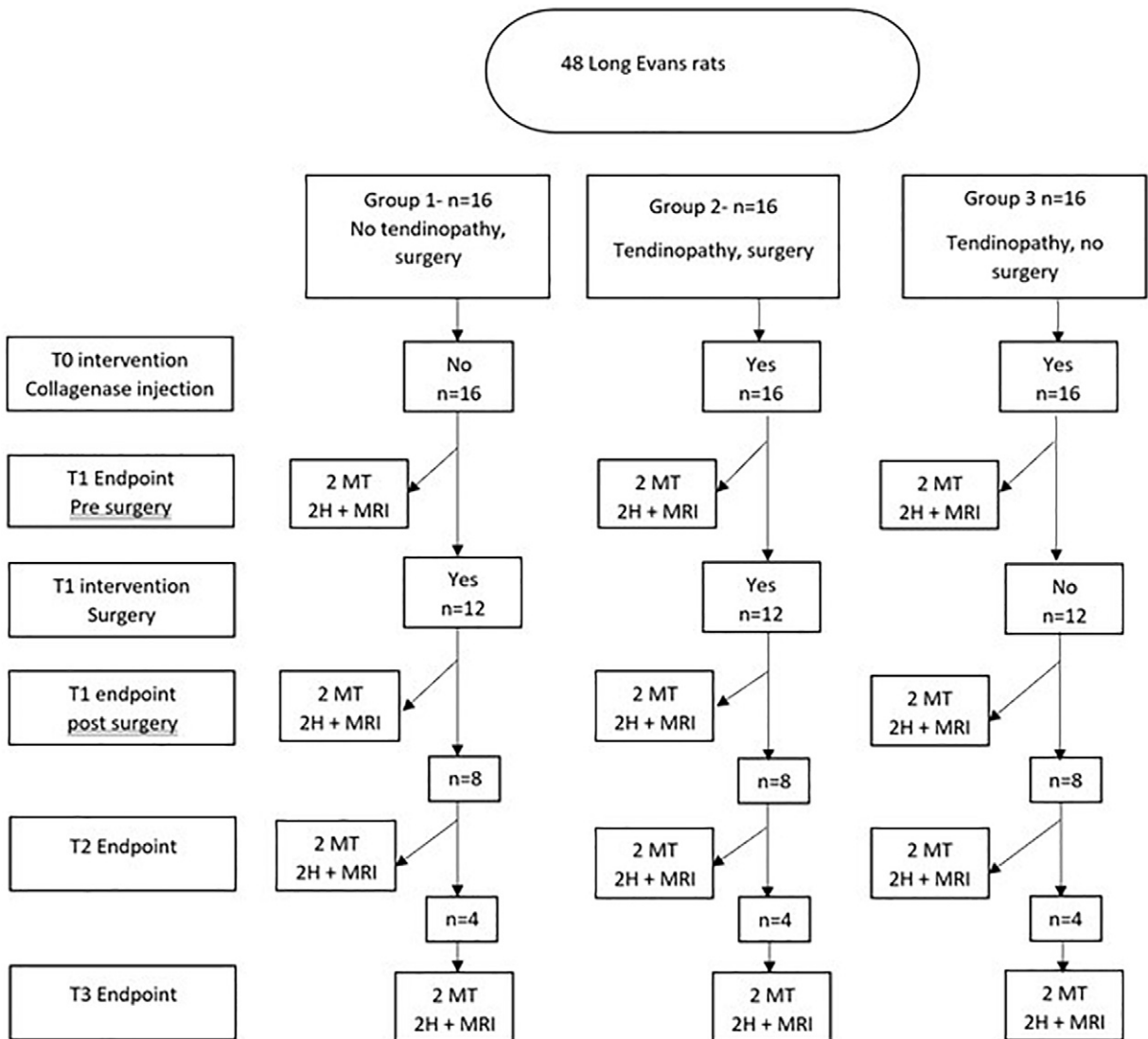


Figure 1. Study flowchart. T0 = time zero when collagenase was injected to those groups allocated to collagenase injection – groups 2 and 3. T1 = one week post collagenase injection, when surgery was performed on those groups it was allocated to groups 1 and 2. Endpoints occurred both immediately before (T1 endpoint pre-surgery) and after surgery (T1 endpoint post-surgery). T2 = endpoint two weeks post collagenase injection (T0) and one week post-surgery (T1), T3 = endpoint four weeks post-surgery (T1), five weeks post collagenase (T0). MT = mechanical testing, H = histology, MRI = magnetic resonance imaging.

standardized regardless of the appearance of the patellar tendon on initial inspection (Figure 2e–g). Routine skin closure was then performed using a buried cruciate suture using 4-0 braided multi-filament suture (Vicryl) (Figure 2e–l).

2.5. Mechanical testing

Specimens allocated for mechanical testing were stripped of all soft tissue prior to testing. The tibia–patella tendon complex was mounted into custom-made jigs and tested using a Mach-1 testing system (Biosyntechn Inc., Montreal, Quebec, Canada). The specimens were loaded to failure at a rate of 50 $\mu\text{m/s}$. Stiffness (linear portion of the load displacement curves) and maximum load to failure were calculated using Mach-1 analysis software. Testing was performed at room temperature and the sample kept hydrated with PBS. Failure mode of the specimens was recorded as the site of the specimen failure: tendon mid substance, tibial enthesis, and patella enthesis.

2.6. Histology

Limbs were isolated and sectioned at the proximal femur and distal tibia knee joint. Specimens were fixed in 10% phosphate-buffered formalin for 48 h. Tissues were decalcified in 10% formic acid–formalin. The knee and patellar tendon complex were sectioned in the sagittal plane at the level of the cruciate ligaments and embedded in paraffin. Five-micrometer sections were cut

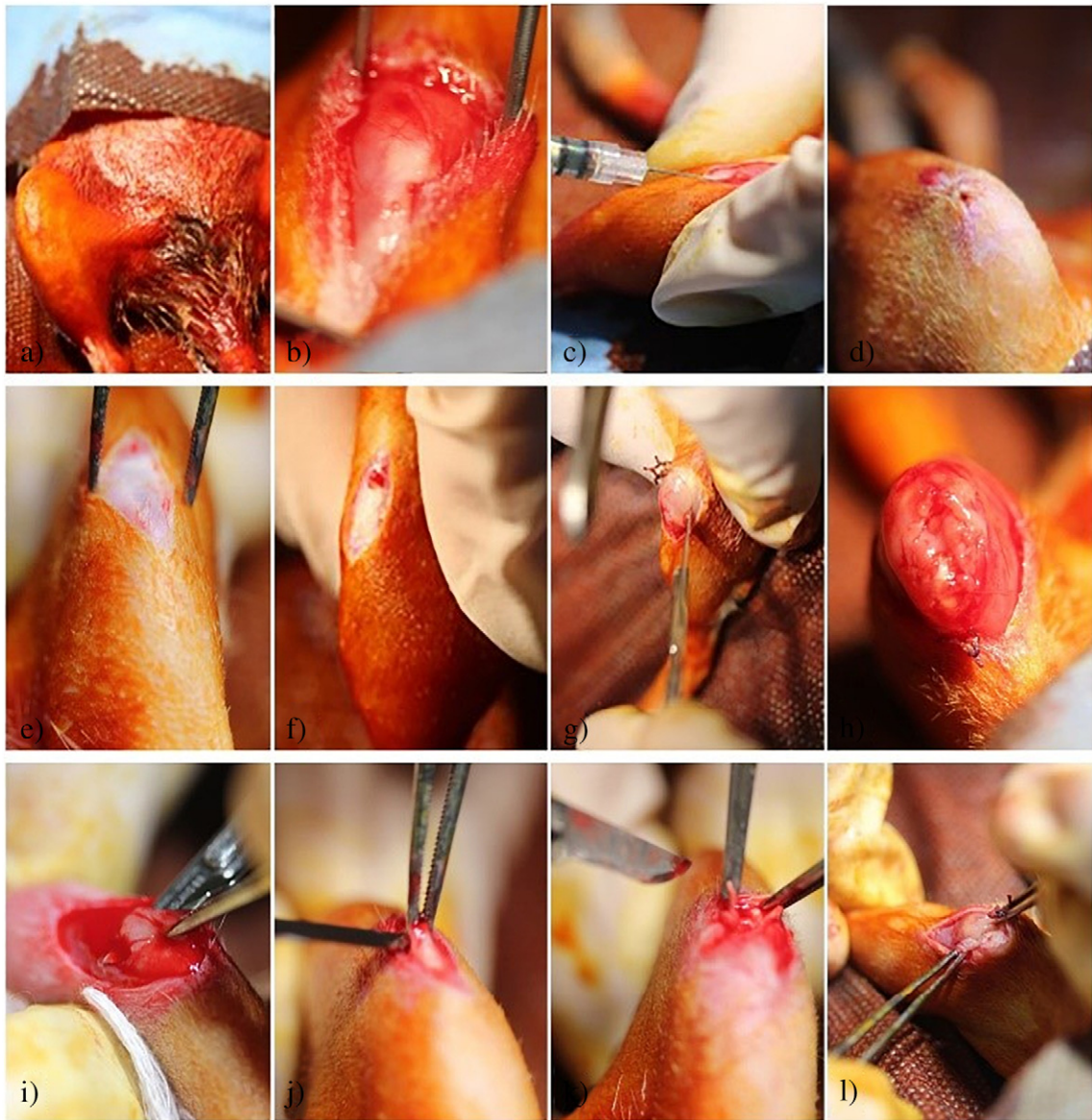


Figure 2. a) Injection and surgical site: sterile preparation and draping. b) Longitudinal incision to directly visualize the patellar tendon–paratenon left intact. c) 29G needle inserted into the patellar tendon, from distal to proximal until the inferior edge of the patella bone was felt, the collagenase was then injected as slowly withdrawing. d) Buried cruciate stitch for meticulous closure. The macroscopic appearance of the patellar tendon at the time of surgical excision varied from e) normal white tendon, f) yellow discoloration, g) inflammatory mass to h) tendon rupture with femoral condyle on show. i–l) Regardless of the appearance, surgical excision was carried out by incising longitudinally medially and laterally on either side of the patellar tendon before placing the no. 15 blade across the tendon to excise the posterior and proximal 1/3.

using a Leica Microtome (Leica Microsystems, Germany) and stained using Harris hematoxylin and eosin. Histology was qualitatively assessed for cellularity, vascularity, and collagen organization in a blinded fashion by two independent observers, quantified with a modified Movin score [20–22] as previously reported Orfei et al. [23] (Table 1).

Prior to formalin fixation, the limbs underwent examination with a 9.4-T MRI (Bruker BioSpin MRI GmbH) at the Mark Wainwright Analytical Centre, UNSW. High resolution T2-weighted fast spin-echo images were acquired of the knee in the sagittal plane. Experimental parameters for these images included: slice thickness = 0.5 mm, spacing between slices = 0.5 mm, repetition time [TR, ms] = 3300, echo time [TE, ms] = 26, number of averages = 6, imaging frequency = 400.34.

2.7. Statistical analysis

Statistical analysis for the quantitative parameters (mechanical testing and histology) between the groups was performed by Analysis of variance (ANOVA) post-hoc Tukey's Honest Significant Difference (HSD) test multiple comparison test to detect

Table 1

Modified Movin Score. Grading system for the tendon histological evaluation.

	0	1	2	3
Fiber structure and arrangement	Normal: continuous, parallel collagen fibers	Slightly abnormal: partially disorganized and fragmented fibers	Abnormal: moderately disorganized, fragmented, crossed and wavy fibers	Markedly abnormal: total disorganized and non-identifiable fiber pattern
Cell density	Normal	Slightly increased	Moderately increased	Markedly increased
Cell appearance	Spindle-shaped cells	Slightly rounded cells	Moderately rounded cells	Markedly rounded cells
Inflammatory cell infiltration	<10%	10–20%	20–30%	>30%
Neovascularization	Normal presence of vascular bundles	Slight increase of vascular bundles	Moderate increase of vascular bundles	Marked increase of vascular bundles
Fatty deposits	Absence of lipid vacuoles	Slight increase of lipid vacuoles	Moderate increase of lipid vacuoles	Marked increase of lipid vacuoles

significant differences between the treatment groups. If the data was not normally distributed, non-parametric Kruskal–Wallis tests were used to compare the treatment effects. Significance was set to an alpha level of $p < 0.05$. All data are presented as the mean and the standard error of the mean. Intraclass correlation coefficients was used to determine the intra- and interobserver reliability for histology grading, with all samples reviewed by two independent graders and 22 random samples reviewed again by one grader. Analysis was performed using SPSS version 18.0 for Windows (SPSS Inc., Chicago, Illinois, USA).

3. Results

Direct vision was used to inject collagenase and provided a more accurate method than ultrasound guided administration due to the small nature of the rat patella tendon. All animals recovered well following the injection of collagenase or surgical intervention.

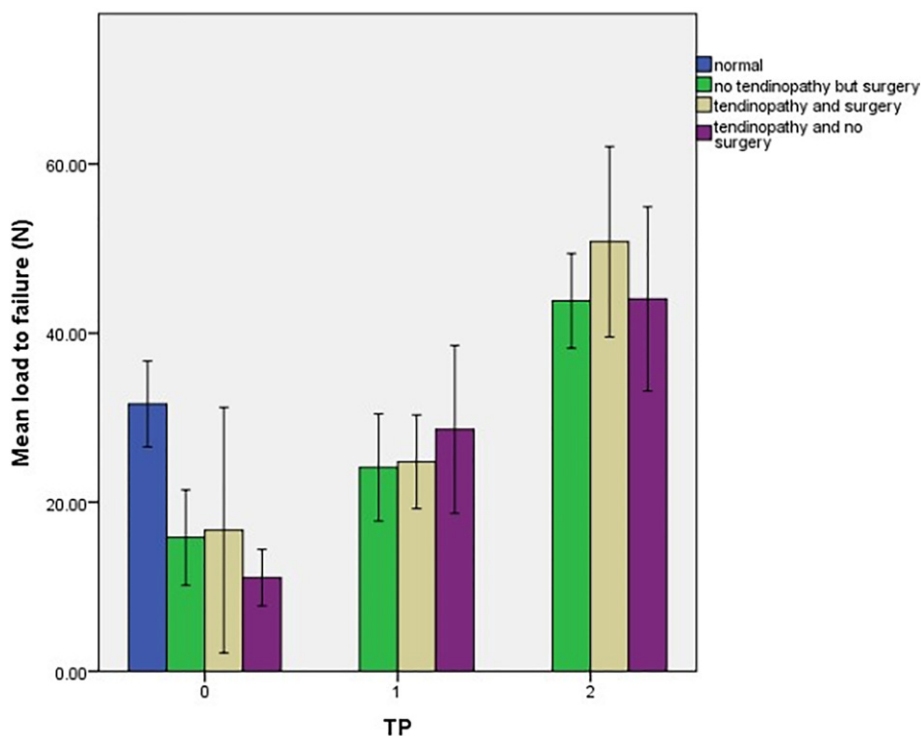


Figure 3. Ultimate load to failure. Ultimate load to failure (Newtons, SE) for each group reported as mean and standard error across time points (TP). Time point 0 = one week post tendinopathy, immediately post-surgical intervention, 1 = two weeks post tendinopathy, one week post-surgical intervention, 2 = five weeks post tendinopathy, four weeks post-surgical intervention.

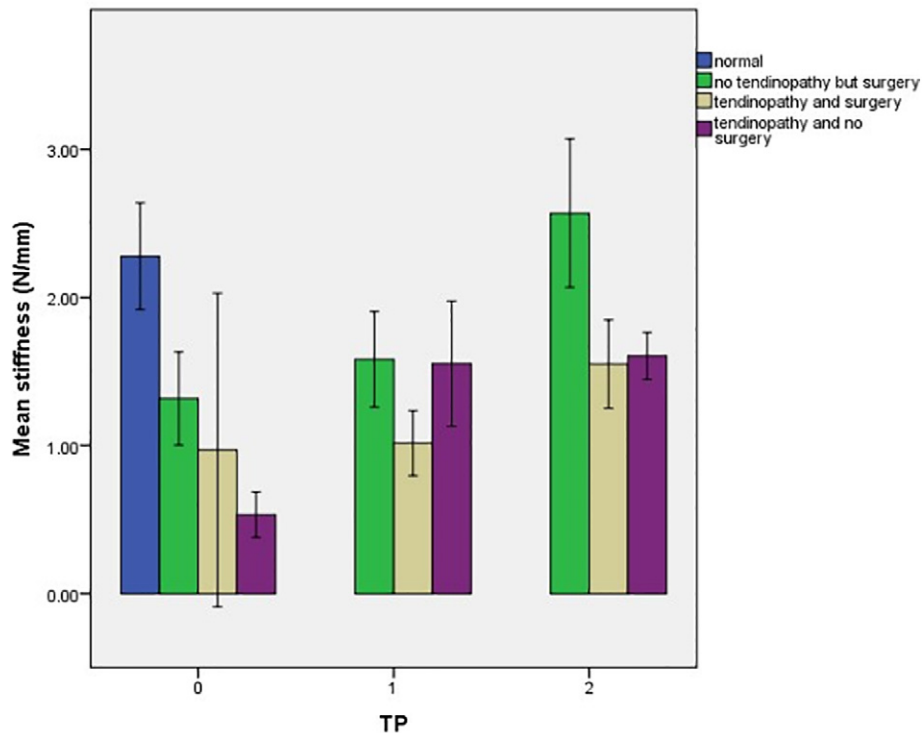


Figure 4. Stiffness. Stiffness (N/mm) for each group reported as mean and standard error across time points (TP). Time point 0 = one week post tendinopathy, immediate post-surgical intervention, 1 = two weeks post tendinopathy, one week post-surgical intervention, 2 = five weeks post tendinopathy, four weeks post-surgical intervention.

3.1. Mechanical testing

There was a mean difference between normal tendons and all the intervention groups ($p < 0.01$) at time 0 for ultimate load to failure. However, there was no difference between the intervention groups at all time points with a mean increase in the load to failure as the time points progressed (Figure 3).

Intact normal tendons were stiffer (N/mm) when compared with all treatment groups studied, ($p < 0.01$). After one week, there was no difference in tendon stiffness between the groups following surgery. After four weeks post-surgery and five weeks following induction of tendinopathy, the no tendinopathy and surgery group (control) were significantly stiffer than both the tendinopathy groups (Figure 4; Table 2).

The point of failure was significantly different between normal tendons, which failed at the inferior pole of the patella, 80% incidence, and mid substance, 20% incidence compared with treated groups, which failed at the mid substance, 90% incidence, ($p < 0.01$) at time point 0. There was no other statistically significant differences in failure point between groups across the time points.

3.2. Histology

The intraclass correlation coefficient for inter-observer reliability was 0.98, and 0.99 for intra-observer reliability. Following induction of tendinopathy, there was an increased number of round and inflammatory cells and loss of parallel orientation of collagen fibers with increased vascularity and fatty deposition with time (Figure 5). Similar changes were noted at the site of the surgical insult in the non-tendinopathy group. There was a substantial improvement with time. This improvement was reflected

Table 2

Mean and standard error for load to failure and stiffness at time points 1) immediately post-surgery, one and four weeks post-surgery.

Time points	No tendinopathy but surgery		Tendinopathy and surgery		Tendinopathy and no surgery	
	Failure (N)	Stiffness (N/mm)	Failure (N)	Stiffness (N/mm)	Failure (N)	Stiffness (N/mm)
Immediately post-surgery	15.82 (2.82)	1.32 (0.16)	16.70 (7.26)	0.97 (0.53)	11.08 (1.67)	0.53 (0.16)
1 week post-surgery	24.12 (3.17)	1.58 (0.16)	24.79 (2.78)	1.02 (0.11)	28.62 (4.97)	1.55 (0.21)
4 weeks post-surgery	43.83 (2.80)	2.57 (0.25)	50.81 (5.63)	1.55 (0.15)	44.05 (5.45)	1.61 (0.08)

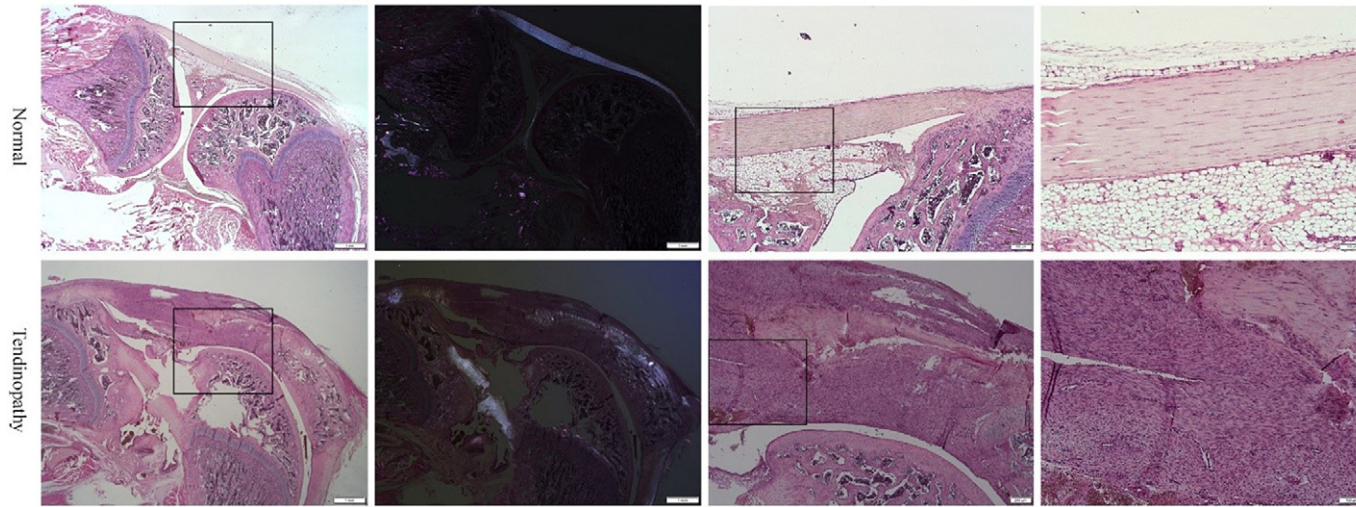


Figure 5. Normal vs tendinopathy tendon. Hematoxylin and eosin staining for normal tendon (top row) and one week post collagenase injection creating tendinopathy (bottom row) at 1.25 \times magnification, polarization, 4 \times and 10 \times magnification (left to right). Note the normal elongated spindle-shaped cells in the normal tendon, compared with the densely populated, disorganized (lack of polarization) plump fibroblastic cells with surrounding lipid vacuoles and neovascularization in the tendinopathy subject. \square demonstrates area of higher magnification.

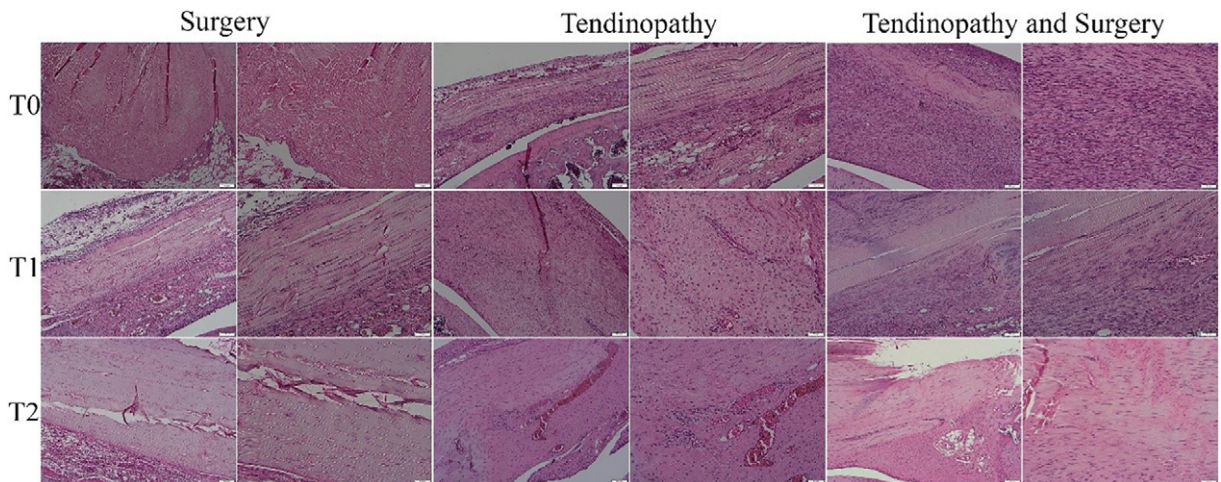


Figure 6. Histology of treatment groups. Hematoxylin and eosin stain for surgical control, tendinopathy alone, and tendinopathy and surgery groups at 10× and 20× magnification. Both surgery and collagenase injection resulted in increased cell density, round plump fibroblastic cells, neovascularization, and lipid vacuoles. In all groups with time, the cell density decreased and the fibroblasts began to elongate. T0 = immediately post-surgical excision and one week post collagenase injection, T1 = one week post-surgical excision and two weeks post collagenase injection, and T2 = four weeks post-surgical excision and five weeks post collagenase injection.

by a decrease in round cells, decrease in the inflammatory response, and increasing numbers of spindle-shaped cells (Figure 6) with reorientation of collagen fibers seen on polarized light.

Normal tendons scored a modified Movin score of 0/18. The surgery resulted in a score of 7.25 (SE 0.29), this was significantly different to both the tendinopathy groups ($p = 0.02$). At one week post tendinopathy injection, the mean score was 11.45 (SE 2.25) for the tendinopathy alone and 12.42 (SE 0.95) for tendinopathy and surgery, with no difference between tendinopathy groups (no surgery vs surgery) ($p = 0.90$). At one week post-surgery, two weeks post tendinopathy injection, there was no difference between the groups. The mean score for the tendinopathy and surgery group was 15 (SE 0.71) compared with 13.25 (SE 0.48) for the tendinopathy group ($p = 0.55$) and 11 (SE 1.78) for the surgical intervention alone group ($p = 0.08$). At four weeks post-surgery, five weeks post tendinopathy injection, there was no statistically significant difference between groups regardless of disease or treatment. This was reflected by a mean score for the tendinopathy and surgery group of 10.5 (SE 1.04), compared with 7.25 (SE 1.65) for the tendinopathy group ($p = 0.26$) and 9.25 (SE 1.31) for the surgical intervention alone group ($p = 0.80$).

3.3. MRI

Figure 7 demonstrates the variable tissue response to collagenase injection and surgical intervention. There was complete loss of the normal black tendon signal replaced with an enlarged high signal mass in its place. At the final time point, there was return of the normal black tendon signal; however, it was thickened and elongated compared with baseline.

4. Discussion

This study explored the basic science behind surgery for tendinopathy utilizing collagenase to simulate tendon pathology in a rat model with biomechanical testing, histology, and MRI. The overarching aim was to improve pathophysiology knowledge of the response to treatment, and thereby to improve treatment and clinical outcomes in patellar tendinopathy patients. We failed to show a difference in the histological response or the mechanical properties of the patellar tendon in rats with tendinopathy who underwent surgical excision compared with those that did not. We demonstrated that surgery alone results in a stiffer tendon, which is weaker in the ultimate load to failure compared with the normal rat tendon. We did not detect any benefit following surgical excision of diseased patellar tendon from both a histological and mechanical strength viewpoint. This finding is in keeping with the lack of high level clinical evidence to support the use of surgical excision. Therefore, we cannot support the use of surgery for tendinopathy based on our findings [4]. The use of high resolution MRI, as reported in this study, points to differences in the rodent model that may limit its applicability to the human condition.

Although high level clinical evidence is lacking [4,5], it is common practice for severe patellar tendinopathy patients to undergo surgical excision when non-operative management has been exhausted [2]. Animal tendinopathy models are utilized to investigate the effect of treatment options on tendinopathy. While we failed to show a beneficial effect of surgery to the histological or mechanical strength of the tendinopathic tendon, the MRI findings of our study show that this model is not reflective of the condition in humans. The MRI findings in humans include ‘blurring’ of ligamentous margins and increased signal intensity within the patellar tendon on both short and long TE sequences [24,25]. All treatment groups demonstrated interruption of the

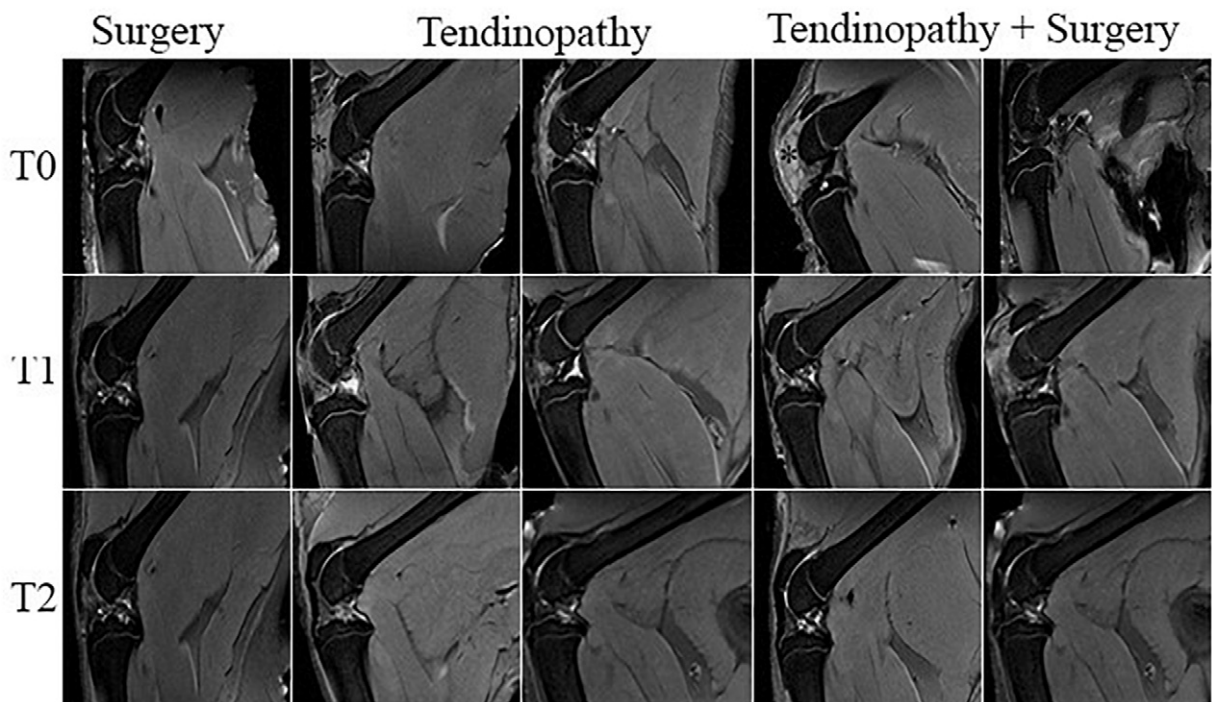


Figure 7. T2-weighted sagittal MRI images of the rat knee at the level of the cruciate ligaments. Demonstrates injection and surgery contained to the patella tendon. Increased signal intensity (* exemplifies this) at the area of the surgical excision (posterior to patella tendon) and collagenase injection. By the end of the study, all tendinopathy subjects healed with thickened and elongated patella tendons. T0 = immediately post-surgical excision and one week post collagenase injection, T1 = one week post-surgical excision and two weeks post collagenase injection, and T2 = four weeks post-surgical excision and five weeks post collagenase injection.

continuity of the patellar tendon, consistent with tendon rupture one week post collagenase injection. Five weeks post induction of tendinopathy, there was complete resolution of tendon integrity with the normal homogenous black tendon signal, regardless of surgical intervention; however, the tendon appeared thickened and elongated.

The MRI findings documented following induction of tendinopathy is an important finding for the use of animal models, in particular for collagenase induced patellar tendinopathy. The rodent collagenase model is an accepted and reported model for the evaluation of patellar tendinopathy, while these models provide a reproducible animal model of patellar tendinopathy based on the immunohistological and histological response to the generation of tendinopathy akin to humans [11–13]. To the authors knowledge, there is only one other study that has utilized MRI imaging in a tendinopathy model. Following ultrasound-guided collagenase injection, Dominguez et al. [14] reported no loss of the characteristic black signal for healthy tendon or change in signal intensity within the tendon but with increased signal intensity within the knee joint and loss of cruciate ligament definition with 7T MRI. This, in conjunction with a lack of cellular change on histology suggests that the injection was given intra-articular and not intra-tendon, which we hypothesize is due to the technically challenging nature of ultrasound-guided injection into the rat patella tendon. During pilot procedures, experienced veterinary and orthopedic surgeons were unsuccessful in accurately and repeatedly injecting methyl blue dye within the tendon under ultrasound guidance. Therefore, we elected to administer the collagenase injection with direct supervision of the tendon, which we feel allows a more accurate delivery. Accuracy of our injection method is reflected in the consistency of histological findings with previously reported studies of tendon injury [23] and containment of MRI changes to the tendon itself rather than the knee joint. Our mechanical data indicates that the collagenase preferentially concentrated its effect within the intrasubstance of the tendon rather than at the patellar tendon–bone enthesis, which our study aimed to reproduce like in humans. Our study demonstrates that while biochemically and histologically, collagenase models are reflective of human tendinopathy [11–13], the MRI appearance is more reflective of tendon rupture and not attune to what is seen in humans; increased signal intensity within the tendon [24]. This may limit the application of the rodent model for future studies.

Our MRI results revealed a complete tendon rupture, which could reflect the dose and concentration of collagenase injection. However, our dose regimen was at the lower end of the reported reference range to induce tendinopathy, with similar modified Movin scores to those reported in the literature [23,26]. Our results support that while the histological and immunohistochemistry may be similar between collagenase models and human tendinopathy [11–13], there is a need to correlate these changes to the MRI findings in order to improve the applicability of animal models to the human condition. Therefore, it is reasonable to question the validity of treatment options for patella tendinopathy derived from animal models [26–30]. More investigation is needed to qualify and quantify the relationship between immunohistochemistry, histology, and MRI of different collagenase models for

different animals to improve the applicability of these models to the human condition before any future preclinical treatment options can be considered of any merit to apply to humans.

The timing of surgical intervention seven days after collagenase was chosen to reflect a median tissue response during the acute injury phase between three and 15 days reported in the literature. The endpoint of one week post-surgery and four weeks post-surgery was designed to examine the acute and chronic surgical response given complete spontaneous resolution occurs by day 45 after injection without treatment [19,23].

A limitation of our study was the reduced numbers in each group per time point to allow for examination of histology and mechanical strength across the study period. However, given the potential limitations of the collagenase model based on our novel MRI investigation, an increase in numbers, based on the reduction and refinement principle [31], may not be warranted until issues with the applicability of the collagenase model have been addressed with further studies correlating the histology findings with MRI. Until animal tendinopathy models have been refined utilizing MRI to show better applicability to humans, its utility as a research tool is limited.

5. Conclusion

In conclusion, we found no difference in the healing response based on mechanical and histological findings to support surgical excision for patellar tendinopathy. While immunohistochemistry and histology may be correlated with human pathogenesis, the 9.4 T MRI findings from our study suggest that applicability of the rat collagenase tendinopathy model to humans is questionable. It is important for the clinician to be aware of the limitations of any animal model when examining research exploring novel treatment options before applying to humans. Further investigation is needed to determine the relationship of MRI changes in animal-based tendinopathy models to facilitate thorough examination of the basic science effect of surgery, and other treatment modalities, for patellar tendinopathy and allow for applicability to humans.

Declaration of competing interest

None.

References

- [1] Kettunen JA, et al. Long-term prognosis for Jumper's knee in male athletes: prospective follow-up study. *Am J Sports Med* 2002;30(5):689–92.
- [2] Figueroa D, Figueroa F, Calvo R. Patellar tendinopathy: diagnosis and treatment. *J Am Acad Orthop Surg* 2016;24(12):e184–92.
- [3] Maffulli N, Longo UG, Denaro V. Novel approaches for the management of tendinopathy. *JBJS* 2010;92(15):2604–13.
- [4] Bahr R, et al. Surgical treatment compared with eccentric training for patellar tendinopathy (Jumper's knee). A randomized, controlled trial. *TJBS* 2006;88(8):1689–98.
- [5] Dan M, Phillips A, Johnston RV, Harris IA. Surgery for patellar tendinopathy (Jumper's knee). *Cochrane Database Syst Rev* 2019(9).
- [6] Brockmeyer M, et al. Results of surgical treatment of chronic patellar tendinosis (Jumper's knee): a systematic review of the literature. *Arthroscopy* 2015;31(12):2424–9.e3.
- [7] Coleman BD, et al. Studies of surgical outcome after patellar tendinopathy: clinical significance of methodological deficiencies and guidelines for future studies. *Victorian Institute of Sport Tendon Study Group. Scand J Med Sci Sports* 2000;10(1):2–11.
- [8] Leadbetter WB, et al. The surgical treatment of tendinitis. Clinical rationale and biologic basis. *Clin Sports Med* 1992;11(4):679–712.
- [9] Sharma P, Maffulli N. Tendon injury and tendinopathy: healing and repair. *JBJS* 2005;87(1):187–202.
- [10] Kader D, et al. Achilles tendinopathy: some aspects of basic science and clinical management. *Br J Sports Med* 2002;36(4):239–49.
- [11] Lake SP, Ansgore HL, Soslosky LJ. Animal models of tendinopathy. *Disabil Rehabil* 2008;30(20–22):1530–41.
- [12] Hast MW, Zuskov A, Soslosky LJ. The role of animal models in tendon research. *BONE JOINT RES* 2014;3(6):193–202.
- [13] Dirks RC, Warden SJ. Models for the study of tendinopathy. *J Musculoskelet Neuronal Interact* 2011;11(2):141–9.
- [14] Dominguez D, et al. Generation of a new model of patellar tendinopathy in rats which mimics the human sports pathology: a pilot study. *Apunts-Med Esport* 2017;52(194):53–9.
- [15] Young MA, et al. Eccentric decline squat protocol offers superior results at 12 months compared with traditional eccentric protocol for patellar tendinopathy in volleyball players. *Br J Sports Med* 2005;39(2):102–5.
- [16] Alfredson H, et al. Heavy-load eccentric calf muscle training for the treatment of chronic Achilles tendinosis. *Am J Sports Med* 1998;26(3):360–6.
- [17] Kaux J-F, et al. Eccentric training improves tendon biomechanical properties: a rat model. *J Orthop Res* 2013;31(1):119–24.
- [18] Visnes H, et al. No effect of eccentric training on Jumper's knee in volleyball players during the competitive season: a randomized clinical trial. *Clin J Sport Med* 2005;15(4):227–34.
- [19] Godbout C, Ang O, Frenette J. Early voluntary exercise does not promote healing in a rat model of Achilles tendon injury. *J Appl Physiol* 2006;101(6):1720–6.
- [20] Maffulli N, et al. Movin and Bonar scores assess the same characteristics of tendon histology. *Clin Orthop Relat Res* 2008;466(7):1605–11.
- [21] Movin T, et al. Tendon pathology in long-standing achillodynia. Biopsy findings in 40 patients. *Acta Orthop* 1997;68(2):170–5.
- [22] Maffulli N, et al. Similar histopathological picture in males with Achilles and patellar tendinopathy. *Med Sci Sports Exerc* 2004;36(9):1470–5.
- [23] Orfei CP, et al. Dose-related and time-dependent development of collagenase-induced tendinopathy in rats. *PLoS one* 2016;11(8):e0161590.
- [24] Johnson DP, Wakeley CJ, Watt I. Magnetic resonance imaging of patellar tendonitis. *Bone Joint J* 1996;78(3):452–7.
- [25] Shalabi A, et al. MR evaluation of chronic Achilles tendinosis: a longitudinal study of 15 patients preoperatively and two years postoperatively. *Acta Radiol* 2001;42(3):269–76.
- [26] Marcos RL, et al. Low-level laser therapy in collagenase-induced Achilles tendinitis in rats: analyses of biochemical and biomechanical aspects. *J Orthop Res* 2012;30(12):1945–51.
- [27] Machova Urdzikova L, et al. Human multipotent mesenchymal stem cells improve healing after collagenase tendon injury in the rat. *Biomed Eng Online* 2014;13:42.
- [28] Casalechi HL, et al. Low-level laser therapy in experimental model of collagenase-induced tendinitis in rats: effects in acute and chronic inflammatory phases. *Lasers Med Sci* 2013;28(3):989–95.
- [29] Yoo SD, et al. Effects of extracorporeal shockwave therapy on nanostructural and biomechanical responses in the collagenase-induced Achilles tendinitis animal model. *Lasers Med Sci* 2012;27(6):1195–204.
- [30] Chen L, et al. Tendon derived stem cells promote platelet-rich plasma healing in collagenase-induced rat achilles tendinopathy. *Cell Physiol Biochem* 2014;34(6):2153–68.
- [31] Grundy D. Principles and standards for reporting animal experiments in the journal of physiology and experimental physiology. *J Physiol* 2015;593(12):2547–9.